

# Hypoxia Promotes Metastasis of Gastric Cancer Through ANXA1 Pathway

**Qing-Hua Liu**

Xuzhou Medical University

**Lei Xia**

Xuzhou Medical University

**Xiao-Yue Wu**

Xuzhou Medical University

**Chen-Chen Lu**

Xuzhou Medical University

**Jing-Yuan Song**

Xuzhou Medical University

**Shisan Bao** (✉ [profbao@hotmail.com](mailto:profbao@hotmail.com))

Xuzhou Medical University

**Ying Liu**

Xuzhou Medical University

---

## Research Article

**Keywords:** HIF1 $\alpha$ , ANXA1, MMP-2, gastric cancer, metastasis

**Posted Date:** October 29th, 2021

**DOI:** <https://doi.org/10.21203/rs.3.rs-1015054/v1>

**License:**  This work is licensed under a Creative Commons Attribution 4.0 International License.

[Read Full License](#)

---

# Abstract

**Background:** To determine the involvement of hypoxia inducible factor 1 $\alpha$  (HIF) pathway in metastasis of gastric cancer (GC).

**Method:** It was determined that the expression of HIF and annexin A1 (ANXA1) in human GC (n=76), using immunohistochemistry, as well as the involvement of HIF pathway in GC cell migration and invasion *in vitro*. The correlation between HIF/ANXA1 and the prognosis was also evaluated.

**Results:** HIF1 $\alpha$  was substantially upregulated in GC tissues, compared to that of non-cancer. HIF1 $\alpha$  was positively correlated with lymph node metastasis, but inversely correlated with survival in GC patients. HIF1 $\alpha$  was an independent prognostic factor in GC patients, and the combination of HIF1 $\alpha$  and ANXA1 might serve as useful prognostic markers in GC patients. Furthermore, HIF-1 $\alpha$  seems to promote GC migration and invasion through HIF1 $\alpha$ /ANXA1/MMP-2 pathway.

**Conclusions:** Our findings suggest that HIF-1 $\alpha$  may serve as a promising prognostic biomarker and therapeutic target for inhibiting GC metastasis.

## Introduction

Gastric cancer (GC) is the fifth most common malignancy tumor worldwide [1] and the second in China [2]. Furthermore, GC is the third leading cause of cancer related death worldwide, and the second in China. The prognosis of GC is not still satisfactory, mainly due to large number of GC patients have been diagnosed at advanced stage with low 5-year survival rate, or even at relative early stage but had distant metastasis, despite extensive development of clinical approaches in surgery and chemotherapy over the last decades [1, 3]. Metastasis is the main cause for the unacceptably high mortality of GC, but the precise underlying mechanism remains to be explored [4, 5].

The tumor microenvironment (TME) plays an important role during tumor metastasis [6, 7]. Hypoxia, a prominent feature of the TME, promotes tumor growth *via* regulating cell growth, apoptosis, survival, angiogenesis, invasion and migration [8], which is supported by the finding that tumor growth is closely related to metastasis under hypoxic TME, resulting in chemoresistance [9]. Furthermore hypoxia inducible factor (HIF) promotes tumor metastasis directly and/or indirectly *via* its downstream pathway [10]. HIF is consisted of one of an O<sub>2</sub> sensitive  $\alpha$  subunits (HIF1 $\alpha$ , HIF-2 $\alpha$ , HIF-3 $\alpha$ ) and is binding to an O<sub>2</sub> sensitive HIF-1 $\beta$  subunit. HIF-1 $\alpha$  is a major regulator of oxygen homeostasis and plays a critical role during the acute adaptation to hypoxia [11], which is also a key transcription factor during the development of malignant [12, 13]. On the other hand, HIF2 $\alpha$  and HIF3 $\alpha$  both have closely related homologues to HIF-1 $\alpha$ . HIF-2 $\alpha$  shares some of biochemical functions with HIF-1 $\alpha$ , but function of HIF-3 $\alpha$  is less clear. In the current study, we focused mainly on the involvement of HIF-1 $\alpha$  in the development of GC.

Annexin A1 (ANXA1), an important downstream protein, is regulated by HIF1 under hypoxia environment [14]. ANXA1, a 37-kDa protein in annexin superfamily, is strongly influencing migration and

invasion of cancer[15–17]. It has been illustrated that the synergistic effect of HIF1 $\alpha$  and ANXA1, showing that HIF-1 $\alpha$  knockout is compensated by upregulating ANXA1 to promote the growth of GC[14]. In addition, HIF-1 $\alpha$ /ANXA1 promote GC proliferation *via* modifying metabolism of GC[14]. However it remains to be explored that the underlying mechanism of HIF1 $\alpha$ /ANXA1 during the development and/or metastasis of GC.

In the current study, we investigated whether hypoxia regulated metastasis of GC *via* HIF1 $\alpha$ /ANXA1 pathway. It was further determined that the correlation between the expression of HIF1 $\alpha$ /ANXA1 in GC tissues and the clinicopathological, as well as, prognostic significance of HIF1 $\alpha$  and ANXA1 in GC patients. Our data suggests that HIF-1 $\alpha$  may act as diagnostic and prognostic marker and potential therapeutic target for GC.

## Results

### The expression of HIF-1 $\alpha$ and ANXA1 in GC and non-tumor tissues

We performed immunohistochemistry with the GC tissue microarray to study whether HIF-1 $\alpha$  and ANXA1 expressions were modified in human GC tissues.

HIF-1 $\alpha$  and ANXA1 were identified in cytoplasm of epithelial cells of both GC and non-GC tissues (Figure 1A). It was observed that HIF-1 $\alpha$ <sup>+</sup> or ANXA1<sup>+</sup> was upregulated by ~ 2.56 fold or 7.89 fold in the GC, compared to that in the non-GC tissues. It is noticed that the absolute value: HIF-1 $\alpha$ <sup>+</sup> or ANXA1<sup>+</sup> was ~ 82.9% or 35.5% in the GC, 32.8% or 4.5% in the non-GC tissues (Figure 1A, Table 1). The result of immunoreactivity scores (IRS) of HIF-1 $\alpha$  and ANXA1 staining available from the GC tissue microarray were consistent with the findings of immunohistochemistry analysis (Figure 1B).

Table 1  
Expression of HIF-1 $\alpha$  and ANXA1 in GC

	HIF-1 $\alpha$		<i>P</i>	ANXA1		<i>P</i>
	+(%)	-(%)		+(%)	-(%)	
None cancer	22(32.8)	45(67.2)	0.000	3(4.5)	64(95.5)	0.000
Cancer	63(82.9)	13(17.1)		27(35.5)	49(64.5)	

HIF-1 $\alpha$  and ANXA1 production was verified in 8 pairs of frozen GC and none cancer gastric tissues, using Western blot. HIF-1 $\alpha$  was 2.0-fold higher in GC than that of non-GC tissue. Similarly, ANXA1 was also 1.4-fold higher in GC tissues than that of non-GC tissues (Figure 1C).

### Correlation between HIF-1 $\alpha$ and clinicopathological parameters in GC patients

Assessment of the association between HIF-1 $\alpha$  expression and the clinicopathological data is presented (Table 2). Increased expression of HIF-1 $\alpha$  was significantly correlated with the diameter of GC ( $P=0.026$ ) and lymph node metastasis ( $P=0.011$ ). There was no significant correlation between HIF-1 $\alpha$  and other clinicopathologic variables, including age, sex, TNM stage, tumor differentiation and hematogenous metastasis. However, there was no significant correlation between ANXA1 and any clinicopathologic variables (Supplementary Table 1).

Table 2  
Comparison of HIF-1 $\alpha$  with Clinicopathological Features in GC patients

Variables	HIF-1 $\alpha$ Staining			<i>P</i>
	Positive(%)	Negative(%)	Total	
Gender				
Male	45(80.4)	11(19.6)	56	0.329
Female	18(90.0)	2(10.0)	20	
Age				
<60	26(78.8)	7(21.2)	33	0.408
$\geq$ 60	37(86.0)	6(14.0)	43	
TNM				
I-II	37(77.1)	11(22.9)	48	0.080
III-IV	26(92.9)	2(7.1)	28	
Tumor Differentiation				
Poor	43(86.0)	7(14.0)	50	0.322
Moderate + Well	20(76.9)	6(23.1)	26	
Tumor Diameter				
$\leq$ 5cm	32(74.4)	11(25.6)	43	0.026
>5cm	31(93.9)	2(6.1)	33	
Lymph Node Metastasis				
Yes	47(90.4)	5(9.6)	52	0.011
No	16(66.7)	8(33.3)	24	
Hematogenous Metastasis				
Yes	9(100.0)	0(0.0)	9	0.149
No	54(80.6)	13(19.4)	67	

# The relationship between HIF-1 $\alpha$ expression and prognosis of GC

To determine whether the expressions of HIF-1 $\alpha$  and ANXA1 in GC patients were correlated with the prognosis of GC patients, GC samples with the IRS of 0-4 were classified as low-expressing, and samples with the IRS of 5-12 were identified as having high HIF-1 $\alpha$  and ANXA1 expressions. High HIF-1 $\alpha$  expression was inversely correlated with overall survival in GC patients ( $P=0.000$ , Figure 1D). However, there was no significant correlation of between ANXA1 and the prognosis of GC patients ( $P=0.107$ , Figure 1D).

Furthermore, to determine whether the expression of HIF-1 $\alpha$  was an independent prognostic marker for GC patients, we analyzed HIF-1 $\alpha$ , sex, age, tumor differentiation, diameter, lymph node metastasis, TNM stage and hematogenous metastasis, using univariate and multivariate Cox regression analysis. Univariate analysis revealed that there was significant correlation between overall survival and HIF-1 $\alpha$ , lymph node metastasis or TNM stage in GC patients ( $P<0.05$ ) (Table 3). Moreover, multivariate analysis revealed that only HIF-1 $\alpha$  was a significant independent prognostic factor in survival of GC patients (Table 3).

Table 3  
Univariate and multivariate analysis of HIF-1 $\alpha$  and clinicopathological factors predicting survival of GC patients

Variables	Univariate analysis		Multivariate analysis	
	HR (95%CI)	<i>p</i> -value	HR (95%CI)	<i>p</i> -value
<b>HIF-1<math>\alpha</math></b>	3.660(1.838-7.288)	0.000	2.750(1.341-5.640)	0.006
<b>Gender</b>	0.828(0.407-1.685)	0.603	-	-
<b>Age</b>	0.794(0.418-1.507)	0.480	-	-
<b>Tumor size (Diameter)</b>				
	1.721(0.904-3.279)	0.098	-	-
<b>Lymph node metastasis</b>				
	0.349(0.159-0.767)	0.009	0.498(0.210-1.182)	0.114
<b>Tumour differentiation</b>				
	0.888(0.446-1.767)	0.735	-	-
<b>Hematogenous Metastasis</b>				
	0.597(0.248-1.435)	0.249	-	-
<b>TNM</b>	2.023(1.052-3.894)	0.035	1.250(0.613-2.545)	0.539

# Relationship between expressions of HIF-1 $\alpha$ and ANXA1 in GC tissues and GC patients

It was determined the correlation between HIF-1 $\alpha$  and ANXA1, showing that the expression of HIF1 $\alpha$  was inversely correlated with ANXA1 in GC tissues ( $P=0.032$ ) (Spearman's rank correlation test) (Table 4). A consistent observation was also observed from Western blot analysis (Figure 1C).

Table 4  
Correlation of HIF-1  $\alpha$  and ANXA1 expression in GC

HIF-1 $\alpha$	ANXA1		Spearman	
	Negative	Positive	Rho	<i>P</i>
Negative	5	8	-0.247	0.032
Positive	44	19		
Sum	49	27		

Kaplan-Meier analysis was further applied to compare overall survival of GC patients, according to combinations of HIF-1 $\alpha$  and ANXA1. GC patients with low HIF-1 $\alpha$  plus low ANXA1 expressions had the longest survival of GC patients ( $P<0.05$ ), while those with high HIF-1 $\alpha$  plus high ANXA1 had worse survival ( $P<0.05$ ) (Figure 1D).

## Hypoxia increases HIF-1 $\alpha$ expression and promotes GC cell migration and invasion

Hypoxia incubation condition was adapted from the publication[18]. It was determined that the expressions of HIF-1 $\alpha$  in GC cell lines (HGC27 and MGC803), as well as, the migration and invasion of GC cells following incubation under hypoxia condition accordingly[18, 19]. HIF-1 $\alpha$ , but not HIF2 $\alpha$ , was upregulated 3.0 or 5.5-fold higher in the hypoxia condition (CoCl<sub>2</sub>) for 6 or 12h, compared to that no non-hypoxia (Figure 2A).

It was further determined that the effects of hypoxia on the migration and invasion of GC cells, using wound healing and transwell assays. It was measured that the width of the scratches in the wound healing at 0, 6 and 12h (Figure 2B), showing that the wound healing in HGC27 or MGC803 cells were faster 1.6 or 1.5 fold under hypoxia condition than that under normoxia condition. The ability of migration was determined in transwell system[20, 21], showing that hypoxia 2.2 or 2.1-fold enhanced the ability of HGC27 or MGC803 cells to migrate through transwell filter inserts compared to that non-hypoxia (Figure 3A). In addition, we further examined the ability of GC invasion under hypoxia, showing that hypoxia significantly 2.1 or 2.5-fold enhanced the ability of HGC27 or MGC803 cells to invade through the transwell filter inserts compared to that non-hypoxia (Figure 3B).

## Hypoxia promotes the migration and invasion of GC cells through HIF1 $\alpha$ /ANXA1/MMP-2 pathway

To investigate the involvement of HIF1 $\alpha$ /ANXA1/MMP-2 pathway under hypoxia condition, it was detected that the protein production of HIF1 $\alpha$ , ANXA1, MMP-2, TIMP-2, MMP-9 and TIMP-1 with the same treatment in HGC27 and MGC803 cells, using Western blot. It was detected that upregulation of HIF1 $\alpha$  and MMP-2, but downregulation of ANXA1 and TIMP-2 in GC cells under hypoxia condition (Figure 4A). It was further explored the activity of MMP-2, using gelatin zymography, showing that the activity of MMP-2 was 1.9-fold increased under hypoxia compared to that non-hypoxia (Figure 4B).

To further validate interaction among HIF1 $\alpha$ , ANXA1 and MMP-2, immunoprecipitation was applied in both HGC27 and MGC803 cells, showing that there was interaction among HIF1 $\alpha$ , ANXA1 and MMP-2 in both HGC27 and MGC803 cells (Figure 4C).

In addition, it was utilized immunofluorescence to identified subcellular localization of HIF1 $\alpha$ , ANXA1 and MMP-2 in these two GC cell lines. HIF1 $\alpha$ , ANXA1 and MMP2 were all localized in the cytosol of GC cells (Figure 5A, 5B). Furthermore, following transfection of ANXA1 siRNA in GC cells (Figure 5C), the expression of MMP-2 was upregulated by 2.3-fold (Figure 5D, 5E). Furthermore, the effect of MMP-2 in the migration and invasion of GC cells was confirmed, using specific MMP2 selective inhibitor (SB-3CT) (Cat No 292605-14-2, MedChemExpress, USA) (Figure 6A). Migration (Figure 6B, 7A) and invasion (Figure 7B) were inhibited by 65% and 60% in the presence of SB-3CT in GC cells.

## Discussion

Hypoxia is defined as the increase in consumption of oxygen or reduction of oxygen relatively to the supply in cells, tissues and organs. Solid tumor cells survived in a microenvironment of hypoxia known as hypoxic adaptation[22]. HIF1 $\alpha$  plays the critical role in tumor hypoxic adaptation and it may mediate series of downstream signaling pathways, involving in tumor metastasis[23] and invasion the extracellular matrix [24]. In our present study, we found the increased expression of HIF1 $\alpha$  in GC was correlated with the diameter of GC and lymph node metastasis, suggesting that HIF1 $\alpha$  promotes the development of GC. Furthermore, increased HIF1 $\alpha$  was correlated with a poor overall survival in GC patients and HIF-1 $\alpha$  was a significant independent prognostic factor in survival of GC patients. In the current study, HIF1 $\alpha$  expression was upregulated substantially on GC cells under CoCl<sub>2</sub> induced hypoxia condition *in vitro*, which also promoted the migration and invasion of GC cells. Our current finding that hypoxia enhanced HIF1 $\alpha$  expression is consistent with upregulated HIF1 $\alpha$  expression on hepatocellular carcinoma cells in response to CoCl<sub>2</sub> induced hypoxia *in vitro*[23, 25].

ANXA1 is an important downstream protein regulated by increased HIF1 $\alpha$  under hypoxia environment[14]. It has been reported that ANXA1 contributes to the progress of tumor metastasis of several human tumors[26, 27]. In addition, ANXA1 inhibits metastasis of breast cancer targeting *via* regulating angiogenesis and NF- $\kappa$ b pathway[28]. HIF1 $\alpha$  also participates in regulating metabolism of GC cells *via* ANXA1[14]. Our current finding demonstrated that the expression of HIF1 $\alpha$  was inversely correlated with ANXA1 in GC tissue, inviting speculation that HIF1 $\alpha$  promotes the development of GC, particularly enhances migration and invasion of GC cell under hypoxia condition *via* inversely regulating ANXA1. Our

speculation was confirmed in the GC cells under hypoxia conditions *in vitro*, showing the interaction among HIF1 $\alpha$  and ANXA1, using immunoprecipitation and immunofluorescence approached, showing that HIF1 $\alpha$  was negatively regulating of ANXA1, which was further confirmed with Western blot. Our observation is also consistent with others, showing that ANXA1 mRNA has been enhanced after HIF1 $\alpha$  loss[14].

Our data demonstrated that the expression and activity of MMP-2 in GC cell lines were significantly upregulated following transfection ANXA1 siRNA, however, while the expression of tissue inhibitors of matrix metalloproteinases (TIMP)-2 was suppressed. Thus our finding suggests that ANXA1 suppresses GC metastasis *via* inhibiting MMP2 activity and subsequently reducing migration and invasion of GC cells. This is line with the others, showing that ANXA1 suppresses tumor metastasis *via* downregulating MMP-9 or MMP-2 in breast cancer[29] or esophageal cancer, respectively[30]. It is well known that MMP-2 and MMP-9 enhance cancer migration and invasion at the early stage of malignant tumor *via* degradation of extracellular matrix (ECM)[31]. TIMP-2 or TIMP-1 is a key regulatory factor in the expressions and activities of MMP-2 or MMP-9 MMPs, respectively[32]. From functional point of view, we further demonstrated that MMP-2 in GC cells was blocked with the selective inhibitor of MMP-2, and consequently inhibited the migration and invasion of GC. Our finding is confirming that the suppressed ANXA1 promoted the development of GC *via* MMP2.

Taken together, our data supports that HIF1 $\alpha$  promotes the migration and invasion of GC *via* inversely regulating downstream ANXA1, but upregulating MMP-2.

## Conclusion

In summary, upregulated HIF1 $\alpha$  in GC was correlated with lymphatic metastasis and poor survival rate of GC patient. HIF-1 $\alpha$  seems to be an independent prognostic factor in GC, and the combination of HIF-1 $\alpha$  and ANXA1 might serve as a useful prognostic markers in GC. Furthermore, HIF-1 $\alpha$  promoted GC migration and invasion through HIF1 $\alpha$ /ANXA1/MMP-2 pathway. Our results may provide new insight for both diagnosis and cellular therapy of GC.

## Methods

### Patients and specimens

Formalin fixed paraffin-embedded GC tissues and the adjacent tissues (control) used for immunohistochemistry were obtained from 76 GC patients undergoing gastrectomy in the Affiliated Hospital, Xuzhou Medical University, China, 2009. The patients were comprised of 56 males and 20 females, aged from 23 to 85 years (Table 1, 2). All of these patients had accepted no chemotherapy in prior to their gastrectomy surgeries. Until May, 2015, 14 out of 76 patients were still alive (the survival period until May 2015 was 62 months); whereas 39 out of 76 patients were dead, and there were 23 patients lost contacted during the following-up.

Frozen samples from 8 pairs of surgically resected GC tissues and their adjacent non-tumor tissues used for Western blot were obtained from GC patients undergoing gastrectomy in the Affiliated Hospital, Xuzhou Medical University, China, 2018.

This study was conducted according to the Declaration of Helsinki principles. This study was approved by the Human Ethical Committee, the Institutional Review Boards of Affiliated Hospital of Xuzhou Medical University (xyfylw2012002), and written informed consents were obtained from all patients, and in case of dead, written informed consents were obtained from next of kin.

## **Immunohistochemistry and Western Blot**

GC tissue microarray was constructed by a precision arraying instrument (Beecher Instruments, Silver Spring, MD, USA). The slides from GC tissue microarray were deparaffinized, rehydrated and heated in sodium citrate buffer (0.01 mol/l, PH 6.0) for 8 min at 95°C. Then, the slides were incubated with 3% hydrogen peroxide for 15 min at room temperature and blocked with normal goat serum (Beijing Sequoia Jinqiao Biological Technology Co., Ltd.). After drained off the blocking serum, the slides were labelled with two antibodies (rabbit anti-HIF-1 $\alpha$  monoclonal antibody: 20960-1-AP, Proteintech Group, Chicago, US; rabbit anti-ANXA1 polyclonal antibody: 21990-1-AP, Proteintech Group, Chicago, US) overnight at 4°C. The slides were rinsed for 10 min in PBS, 3 times and incubated for 30 min with the HRP-labeled polymer conjugated secondary antibody (12127A07, Beijing Sequoia Jinqiao Biological Technology Co., Ltd.). The dilution for both antibodies was 1:400. The specific target(s) was visualized with 3, 3'-diaminobenzidine (DAB) detection kit (Beijing Sequoia Jinqiao Biological Technology Co., Ltd.) and counterstained with hematoxylin[33].

Positive HIF-1 $\alpha$  and ANXA1 staining appeared brown in cytoplasm with or without in nucleus. We graded positive staining according to both the stain intensity and the percentage of stained cells. Two pathologists independently examined all slides. The intensities of HIF-1 $\alpha$  and ANXA1 staining were scored 0 to 3 (0=negative, 1=moderate; 3=strong). The percentage of stained cells was scored 1 to 4: 1 (0-25% cells positively stained), 2 (26-50%), 3 (51-75%) and 4 (76-100%). Final scores of both two proteins positive staining were evaluated by the immunoreactive score (IRS), which was calculated by multiplying the intensity score by the percentage score of positive cells. The negative staining of the specimens was IRS: 0.

Protein expressions were also evaluated by Western blotting. Equivalent amounts of total proteins from frozen samples of surgically resected GC tissues and their adjacent non-tumor tissues were extracted as according to the extraction protocol of the total protein kit, KeyGen Biotech, China). The concentration determined using BCA protein kit, Beyotime Biotechnology, Shanghai, China. The procedure of western blot analysis was performed as described previously[34]. Protein samples were denatured, electrophoresed in SDS/polyacrylamide gels, and transferred into polyvinylidene difluoride membranes (Millipore). After transfer, the membrane was cut according to the position of the target protein labeled by marker. Antibodies against the following proteins were used: HIF-1 $\alpha$  at a 1:2,000 dilution, ANXA1 at 1:1,000 and anti- $\beta$ -actin at 1:5,000. After incubation with secondary antibody: horseradish peroxidase-

conjugated goat anti-rabbit IgG (ABL3012, AbSci, Washington,US) at a dilution of 1:10,000, protein bands were exposed to ECL system.

## Cell lines

The human GC cell lines HGC27[35] and MGC803[36] were kindly donated from the Shanghai Institute of Biochemistry and Cell Biology, Chinese Academy of Science (Shanghai, China). HGC27 cells were cultured in Roswell Park Memorial Institute 1640 medium (RPMI 1640, Gibco, California, US) supplemented with 10% fetal calf serum (Hangzhou Sijiqing bioengineering Material Co., Ltd, Hangzhou, China); MGC803 cells were cultured in minimum essential medium (MEM, Gibco, California, US) supplemented with 10% fetal calf serum. These two cell lines were both incubated in a 37°C humidified incubator with 5% CO<sub>2</sub>.

The hypoxia condition was established using Cobalt chloride module (CoCl<sub>2</sub>, Sigma-Aldrich, St. Louis, MO, USA) (300µmol/L) in their culture medium as described in other publications[18, 19]

ANXA1 siRNA (5'-CCCGUUCUGAAAUUGACAUTT-3') and nonspecific control siRNA (5'-UUCUCCGAACGUGUCACGUTT-3') were purchased from GenePharma (Suzhou, China). The control and ANXA1 siRNA were transfected into HGC27 and MGC803 cells with Lipofectamine 2000 reagent (Invitrogen, Shanghai, China) according to the manufacturer's instructions.

## Western blot

Proteins from cells were extracted by the same procedure as described previously[34]. The procedure of western blot was the same as above: extracted proteins from cells, antibodies of HIF-1α, ANXA1 and β-actin. HIF-2α (1:2000, DF2928, Affinity Biosciences [Ohio] US), MMP-2 (1:1000, 10373-2-AP, Proteintech Group, Chicago, US), TIMP-2 (tissue inhibitor of metalloproteinase 2) (1:1000, 17353-1-AP, Proteintech Group), MMP-9 (Matrix metal proteinase 9) (1:1000, 10375-2-AP, Proteintech Group), TIMP-1 (tissue inhibitor of metalloproteinase 1) (1:1000, 10753-1-AP, Proteintech Group).

## Gelatin zymography

Gelatin zymography was used to detect the activity of MMP-2. Cells ( $2.5 \times 10^6$ ) were seeded in 100-mm plates and cultured for 3 h, 12 h and 24 h. Then, proteins were collected and concentrated by Amicon Ultra-4-30 k centrifugal filters (Millipore, Billerica, MA, USA), 7500 g, 20 min, at 4°C. We loaded 50µg of protein in non-denaturing conditions into 8% polyacrylamide gel containing 0.1% gelatin (China Pharmaceutical Shanghai chemical reagent station, Shanghai, China). After electrophoresis, gels were washed by 2.5% Triton X-100, 30 minutes. Then, gels were incubated for 48h, 37°C in incubation buffer (50 mM Tris-HCl (pH 8.8), 5 Mm CaCl<sub>2</sub>, 1 µM ZnCl<sub>2</sub>, and 0.02% NaN<sub>3</sub>), stained with Coomassie brilliant blue R-250 for 30 min (Coomassie Blue Staining Kit, Biotechnology Bioengineering Co., Ltd., Shanghai, China) following the steps provided by the manufacturer, and destained in destained solution for 15min, 3 times. The gelatinolytic activities were shown as clear areas in gel. Then, gels were photographed and quantitatively measured by scanning densitometry.

# Co-immunoprecipitation

All operations are carried out at low temperature. Gastric cancer cells HGC27 and MGC803 were cultured under hypoxia condition for 6 h and then were harvested. The cells were lysed with IP RIPA on ice for 30 min.

The lysates were collected by centrifuge at 12,000 rpm for 15 min at 4°C and the supernatant was the total protein. Add PBS to dilute the total protein to 1 µg/µl, and incubate overnight with 1µg HIF-1α antibody for every 500 µg total protein. 30µl protein A/G agarose beads (SC-2003, Santa Cruz Biotechnology, California, US) were added to the cell lysate and incubated at 4 °C for 4 h. The beads were washed 3 times in IP RIPA and subjected to Western blotting.

In order to detect the interaction between HIF-1 and ANXA1, and between HIF-1 and MMP-2, we incubated with antibodies of ANXA1 and MMP-2 respectively during the Western blotting[37].

## Immunofluorescence staining

Identify the location of HIF-1α, ANXA1 and MMP-2 in GC cells by Immunofluorescence staining. Exponentially growing cells were seeded on glass slides in 12-well plates and were cultured in normoxic conditions to CoCl<sub>2</sub> in their culture medium for 6h. The treated cells were rinsed three times with 0.01 M PBS, and fixed for 20 min with 4% paraformaldehyde at 4°C. Afterwards, cells were permeabilized with 0.5% TritonX-100 for 15 min. Later, cells were blocked with 10% normal goat serum for 1h. Primary antibodies: 100 µl /well HIF-1α (1:300) and ANXA1 (1:300) mixture or MMP-2 (1:300) and ANXA1 (1:300) mixture were added and incubated at 4°C overnight. After cells were rinsed with cold PBS three times, the secondary antibody was added and incubated at room temperature for 30min. Subsequently, the slides were stained with 100 µl /well the corresponding Alexa Fluor 488 goat anti-rabbit IgG antibody (VA018, VICMED Life Sciences, Xu Zhou, China) and Alexa Fluor 594 goat anti-mouse IgG (VA019, VICMED Life Sciences, Xu Zhou, China) mixture at room temperature in dark for 1h. The nuclei were stained with 50µl/well 6-diamidino-2-phenylindole (DAPI) at room temperature in dark for 5min. Then, the slides were rinsed with PBS for 5 min, 3 times. Finally, the slides were analyzed by fluorescence microscope (Olympus BX-51, Olympus Corporation, Japan). All samples were processed in parallel.

## Wound healing assay

Wound healing assay was used to detect the ability of cell migration. After transfecting HGC27 and MGC803 cells with ANXA1 siRNA and control siRNA, cells were grown to confluency, wound lines were made by scraping closed Pasteur pipette tips across the confluent cell layer. Then, cells were washed by PBS three times to remove detached cells and debris. The width of wound was observed and measured after 0, 6 and 12 hours[21].

## Cell migration and invasion assays

Cell migration and invasion assays were performed by using modified two chamber migration and invasion assays with a pore size of 8 µm. Transwell filters were inserted with or without Matrigel (BD

Biosciences, USA) coating for invasion and migration assays, respectively. The detailed conditions have been described previously[38].

## Statistical analysis

Data has been expressed as the means  $\pm$  SDs from at least three independent repeats. One-way analysis of variance (ANOVA) and multi-factorial ANOVA were used for comparing the differences between groups. Statistical analysis for the GC tissue microarray was performed by SPSS 16.0. The association between the staining of HIF-1 $\alpha$ , ANXA1 and the clinicopathological parameters of GC patients, including gender, age, tumor size, TNM stage, lymph node and hematogenous metastasis were evaluated by the two-sided Fisher's exact test. The correlation between HIF-1 $\alpha$ , ANXA1 expressions and patient survival was assessed by Kaplan- Meier and log-rank tests. Analysis of univariate and multivariate was analyzed by Cox regression model. Difference was considered significant when  $P < 0.05$ .

## Declarations

### Fundings

This study was funded by grants from the national Natural Science Foundation of China (NO. 81502030), XuZhouScience and Technology Program (KC20138) and theNaturalScienceFoundationoftheJiangsuHigherEducationInstitutionsofChina(18KJA320013).

### Competing interests

The authors declare no competing interest.

### Data availability

All the data will be made available upon request.

### Authors' contributions

Qing-Hua Liu designed the study and performed the experiments; Lei Xia performed the experiments and drafted the figures; Chen-Chen Lu performed the experiments; Ying Liu designed the study and revised the manuscript; Xiao-Yue Wu, Jing-Yuan Song completed the supplementary experiments of Western blot and Gelatin zymography. Shisan Bao revised the manuscript. All authors read and approved the final manuscript.

### Ethics approval and consent to participate

This study was approved by the Human Ethical Committee, the Institutional Review Boards of Affiliated Hospital of Xuzhou Medical University, and written informed consents were obtained from all patients, and in case of dead, written informed consents were obtained from next of kin.

## References

- [1] J. Ferlay, I. Soerjomataram, R. Dikshit, S. Eser, C. Mathers, M. Rebelo, D.M. Parkin, D. Forman, F. Bray, Cancer incidence and mortality worldwide: sources, methods and major patterns in GLOBOCAN 2012, *Int J Cancer*, 136 (2015) E359-386.
- [2] W. Chen, R. Zheng, P.D. Baade, S. Zhang, H. Zeng, F. Bray, A. Jemal, X.Q. Yu, J. He, Cancer statistics in China, 2015, *CA Cancer J Clin*, 66 (2016) 115-132.
- [3] T. Zurleni, E. Gjoni, M. Altomare, S. Rausei, Conversion surgery for gastric cancer patients: A review, *World J Gastrointest Oncol*, 10 (2018) 398-409.
- [4] J.H. Lee, K.K. Chang, C. Yoon, L.H. Tang, V.E. Strong, S.S. Yoon, Lauren Histologic Type Is the Most Important Factor Associated With Pattern of Recurrence Following Resection of Gastric Adenocarcinoma, *Annals of surgery*, 267 (2018) 105-113.
- [5] Y. Hirotsu, M. Hada, K. Amemiya, T. Oyama, H. Mochizuki, M. Omata, Multi-regional sequencing reveals clonal and polyclonal seeding from primary tumor to metastases in advanced gastric cancer, *J Gastroenterol*, 55 (2020) 553-564.
- [6] D. Hanahan, L.M. Coussens, Accessories to the crime: functions of cells recruited to the tumor microenvironment, *Cancer Cell*, 21 (2012) 309-322.
- [7] S. Petanidis, K. Domvri, K. Porpodis, D. Anestakis, L. Freitag, W. Hohenforst-Schmidt, D. Tsavlis, K. Zarogoulidis, Inhibition of kras-derived exosomes downregulates immunosuppressive BACH2/GATA-3 expression via RIP-3 dependent necroptosis and miR-146/miR-210 modulation, *Biomed Pharmacother*, 122 (2020) 109461.
- [8] M.C. Bosco, G. D'Orazi, D. Del Bufalo, Targeting hypoxia in tumor: a new promising therapeutic strategy, *J Exp Clin Cancer Res*, 39 (2020) 8.
- [9] G.L. Semenza, The hypoxic tumor microenvironment: A driving force for breast cancer progression, *Biochim Biophys Acta*, 1863 (2016) 382-391.
- [10] P. Vaupel, A. Mayer, Hypoxia-Driven Adenosine Accumulation: A Crucial Microenvironmental Factor Promoting Tumor Progression, *Adv Exp Med Biol*, 876 (2016) 177-183.
- [11] J.A. Smythies, M. Sun, N. Masson, R. Salama, P.D. Simpson, E. Murray, V. Neumann, M.E. Cockman, H. Choudhry, P.J. Ratcliffe, D.R. Mole, Inherent DNA-binding specificities of the HIF-1 $\alpha$  and HIF-2 $\alpha$  transcription factors in chromatin, *EMBO reports*, 20 (2019).
- [12] T.T. Wei, Y.T. Lin, S.P. Tang, C.K. Luo, C.T. Tsai, C.T. Shun, C.C. Chen, Metabolic targeting of HIF-1 $\alpha$  potentiates the therapeutic efficacy of oxaliplatin in colorectal cancer, *Oncogene*, 39 (2020) 414-427.

- [13] M.C. Lin, J.J. Lin, C.L. Hsu, H.F. Juan, P.J. Lou, M.C. Huang, GATA3 interacts with and stabilizes HIF-1 $\alpha$  to enhance cancer cell invasiveness, *Oncogene*, 36 (2017) 4243-4252.
- [14] N. Rohwer, F. Bindel, C. Grimm, S.J. Lin, J. Wappler, B. Klinger, N. Blüthgen, I. Du Bois, B. Schmeck, H. Lehrach, M. de Graauw, E. Goncalves, J. Saez-Rodriguez, P. Tan, H.I. Grabsch, A. Prigione, S. Kempa, T. Cramer, Annexin A1 sustains tumor metabolism and cellular proliferation upon stable loss of HIF1A, *Oncotarget*, 7 (2016) 6693-6710.
- [15] A. Emmanouilidi, D. Paladin, D.W. Greening, M. Falasca, Oncogenic and Non-Malignant Pancreatic Exosome Cargo Reveal Distinct Expression of Oncogenic and Prognostic Factors Involved in Tumor Invasion and Metastasis, *Proteomics*, 19 (2019) e1800158.
- [16] X. Guan, Y. Fang, J. Long, Y. Zhang, Annexin 1-nuclear factor-kappaB-microRNA-26a regulatory pathway in the metastasis of non-small cell lung cancer, *Thorac Cancer*, 10 (2019) 665-675.
- [17] R. Belvedere, V. Bizzarro, A. Popolo, F. Dal Piaz, M. Vasaturo, P. Picardi, L. Parente, A. Petrella, Role of intracellular and extracellular annexin A1 in migration and invasion of human pancreatic carcinoma cells, *BMC Cancer*, 14 (2014) 961.
- [18] E. Gervin, B. Shin, R. Opperman, M. Cullen, R. Feser, S. Maiti, M. Majumder, Chemically Induced Hypoxia Enhances miRNA Functions in Breast Cancer, *Cancers (Basel)*, 12 (2020).
- [19] J. Zheng, X. Zhu, Y. He, S. Hou, T. Liu, K. Zhi, T. Hou, L. Gao, CircCDK8 regulates osteogenic differentiation and apoptosis of PDLSCs by inducing ER stress/autophagy during hypoxia, *Ann N Y Acad Sci*, 1485 (2021) 56-70.
- [20] B. Wu, K. Hu, S. Li, J. Zhu, L. Gu, H. Shen, B.D. Hambly, S. Bao, W. Di, Dihydroartemisinin inhibits the growth and metastasis of epithelial ovarian cancer, *Oncol Rep*, 27 (2012) 101-108.
- [21] B. Wu, S. Li, L. Sheng, J. Zhu, L. Gu, H. Shen, D. La, B.D. Hambly, S. Bao, W. Di, Metformin inhibits the development and metastasis of ovarian cancer, *Oncol Rep*, 28 (2012) 903-908.
- [22] Q.S. Wu, P.S. Liu, C.P. Yang, Y.B. Chen, [A Review of High-altitude Hypoxia Adaptation and Hypoxic Solid Tumor], *Sichuan Da Xue Xue Bao Yi Xue Ban*, 52 (2021) 50-56.
- [23] B. Feng, Y. Zhu, C. Sun, Z. Su, L. Tang, C. Li, G. Zheng, Basil polysaccharide inhibits hypoxia-induced hepatocellular carcinoma metastasis and progression through suppression of HIF-1 $\alpha$ -mediated epithelial-mesenchymal transition, *Int J Biol Macromol*, 137 (2019) 32-44.
- [24] C.C. Wong, A.K. Kai, I.O. Ng, The impact of hypoxia in hepatocellular carcinoma metastasis, *Front Med*, 8 (2014) 33-41.
- [25] S. Carbajo-Pescador, R. Ordoñez, M. Benet, R. Jover, A. García-Palomo, J.L. Mauriz, J. González-Gallego, Inhibition of VEGF expression through blockade of Hif1 $\alpha$  and STAT3 signalling mediates the

anti-angiogenic effect of melatonin in HepG2 liver cancer cells, *British journal of cancer*, 109 (2013) 83-91.

[26] J. Feng, S.S. Lu, T. Xiao, W. Huang, H. Yi, W. Zhu, S. Fan, X.P. Feng, J.Y. Li, Z.Z. Yu, S. Gao, G.H. Nie, Y.Y. Tang, Z.Q. Xiao, ANXA1 Binds and Stabilizes EphA2 to Promote Nasopharyngeal Carcinoma Growth and Metastasis, *Cancer Res*, 80 (2020) 4386-4398.

[27] C. Guo, S. Liu, M.Z. Sun, Potential role of Anxa1 in cancer, *Future Oncol*, 9 (2013) 1773-1793.

[28] D. Anbalagan, G. Yap, Y. Yuan, V.K. Pandey, W.H. Lau, S. Arora, P. Bist, J.S. Wong, G. Sethi, P.M. Nissom, P.E. Lobie, L.H. Lim, Annexin-A1 regulates microRNA-26b\* and microRNA-562 to directly target NF-kappaB and angiogenesis in breast cancer cells, *PLoS One*, 9 (2014) e114507.

[29] H. Kang, J. Ko, S.W. Jang, The role of annexin A1 in expression of matrix metalloproteinase-9 and invasion of breast cancer cells, *Biochem Biophys Res Commun*, 423 (2012) 188-194.

[30] C. Hu, J. Peng, L. Lv, X. Wang, Y. Zhou, J. Huo, D. Liu, miR-196a regulates the proliferation, invasion and migration of esophageal squamous carcinoma cells by targeting ANXA1, *Oncol Lett*, 17 (2019) 5201-5209.

[31] Y.A. DeClerck, A.M. Mercurio, M.S. Stack, H.A. Chapman, M.M. Zutter, R.J. Muschel, A. Raz, L.M. Matrisian, B.F. Sloane, A. Noel, M.J. Hendrix, L. Coussens, M. Padarathsingh, Proteases, extracellular matrix, and cancer: a workshop of the path B study section, *Am J Pathol*, 164 (2004) 1131-1139.

[32] S. Lenglet, F. Mach, F. Montecucco, Role of matrix metalloproteinase-8 in atherosclerosis, *Mediators of inflammation*, 2013 (2013) 659282.

[33] R. Puranik, O.J. Fox, D.S. Sullivan, J. Duflou, S. Bao, Inflammatory characteristics of premature coronary artery disease, *Int J Cardiol*, 145 (2010) 288-290.

[34] Q.H. Liu, H.M. Yong, Q.X. Zhuang, X.P. Zhang, P.F. Hou, Y.S. Chen, M.H. Zhu, J. Bai, Reduced expression of annexin A1 promotes gemcitabine and 5-fluorouracil drug resistance of human pancreatic cancer, *Invest New Drugs*, 38 (2020) 350-359.

[35] L. Zhang, Z.P. Yan, Z.H. Hou, P. Huang, M.J. Yang, S. Zhang, S. Zhang, S.H. Zhang, X.L. Zhu, C.F. Ni, Q. Li, Neutrophil-to-Lymphocyte and Platelet-to-Lymphocyte Ratios as Predictors of Outcomes in Patients With Unresectable Hepatocellular Carcinoma Undergoing Transarterial Chemoembolization Plus Sorafenib, *Frontiers in molecular biosciences*, 8 (2021) 624366.

[36] Q. Wang, Y. Tang, T. Wang, H.L. Yang, X. Wang, H. Ma, P. Zhang, EPCR promotes MGC803 human gastric cancer cell tumor angiogenesis in vitro through activating ERK1/2 and AKT in a PAR1-dependent manner, *Oncol Lett*, 16 (2018) 1565-1570.

[37] K.K. Dey, R. Bharti, G. Dey, I. Pal, Y. Rajesh, S. Chavan, S. Das, C.K. Das, B.C. Jena, P. Halder, J.G. Ray, I. Kulavi, M. Mandal, S100A7 has an oncogenic role in oral squamous cell carcinoma by activating p38/MAPK and RAB2A signaling pathway, *Cancer gene therapy*, 23 (2016) 382-391.

[38] Q.H. Liu, M.L. Shi, J. Bai, J.N. Zheng, Identification of ANXA1 as a lymphatic metastasis and poor prognostic factor in pancreatic ductal adenocarcinoma, *Asian Pacific journal of cancer prevention : APJCP*, 16 (2015) 2719-2724.

## Figures

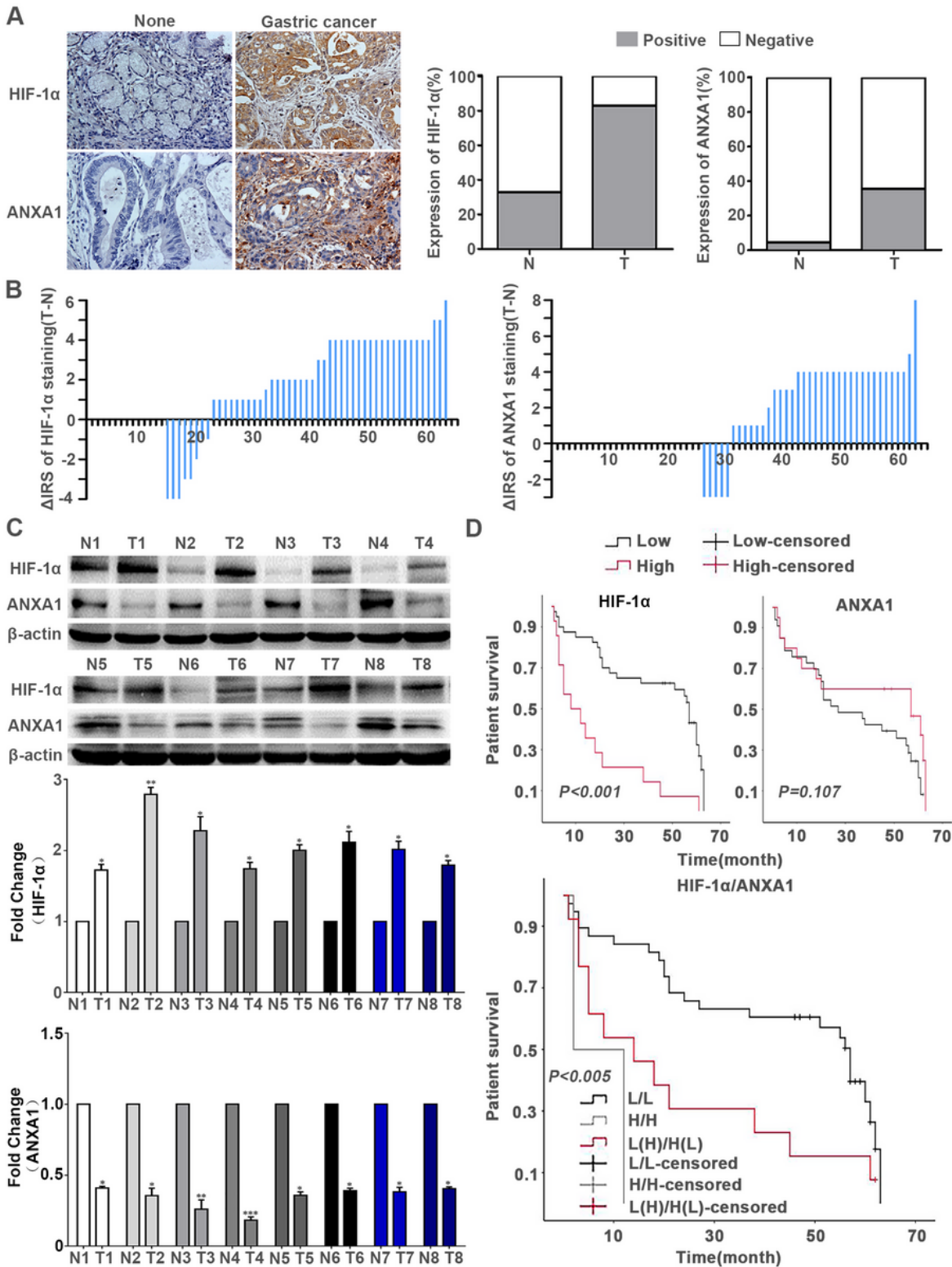


**Figure 1**

HIF-1 $\alpha$  is increased in GC and associated with overall survival in GC patients. (A) Top panel, HIF-1 $\alpha$  and ANXA1 immunohistochemical staining in GC and normal gastric tissues,  $\times 400$ . (B) Distributions of the difference HIF-1 $\alpha$  and ANXA1 staining in in GC and normal gastric tissues were available from the 62 pairs of tissues. (C) The expression of HIF-1 $\alpha$  was high versus low expression of ANXA1 determined by

Western blot in 8 pairs of the same frozen gastric tissues. (D) High expression of HIF-1 $\alpha$  correlated with worse overall survival. The combination of high HIF-1 $\alpha$  plus high ANXA1 had worse overall survival.

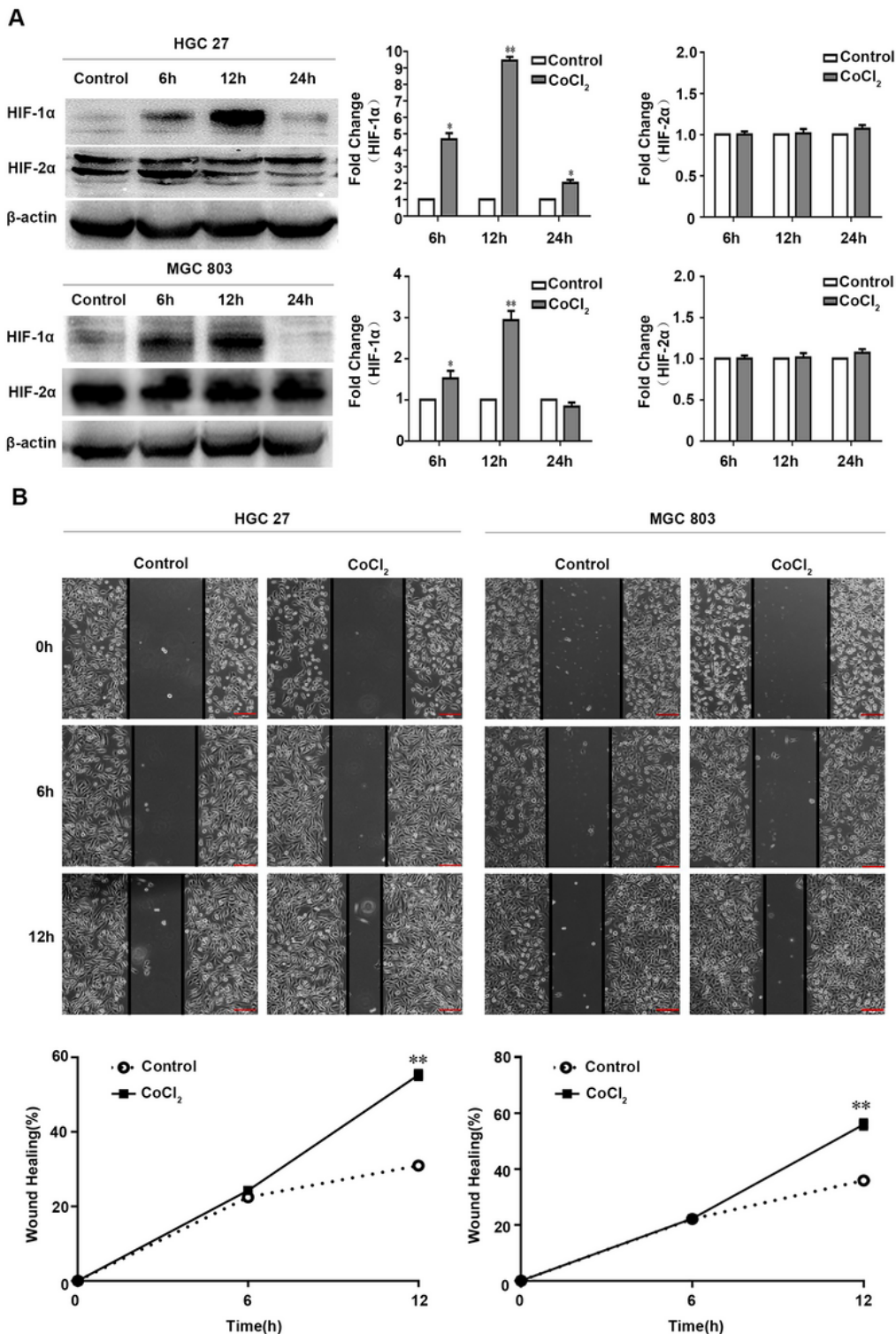


**Figure 2**

HIF-1 $\alpha$  improves wound healing of GC cells. (A) The expression of HIF-1 $\alpha$  was significantly increased in both HGC27 and MGC803 cells after 6h and 12h co-cultured with CoCl<sub>2</sub>. The expression of HIF-2 $\alpha$  was no



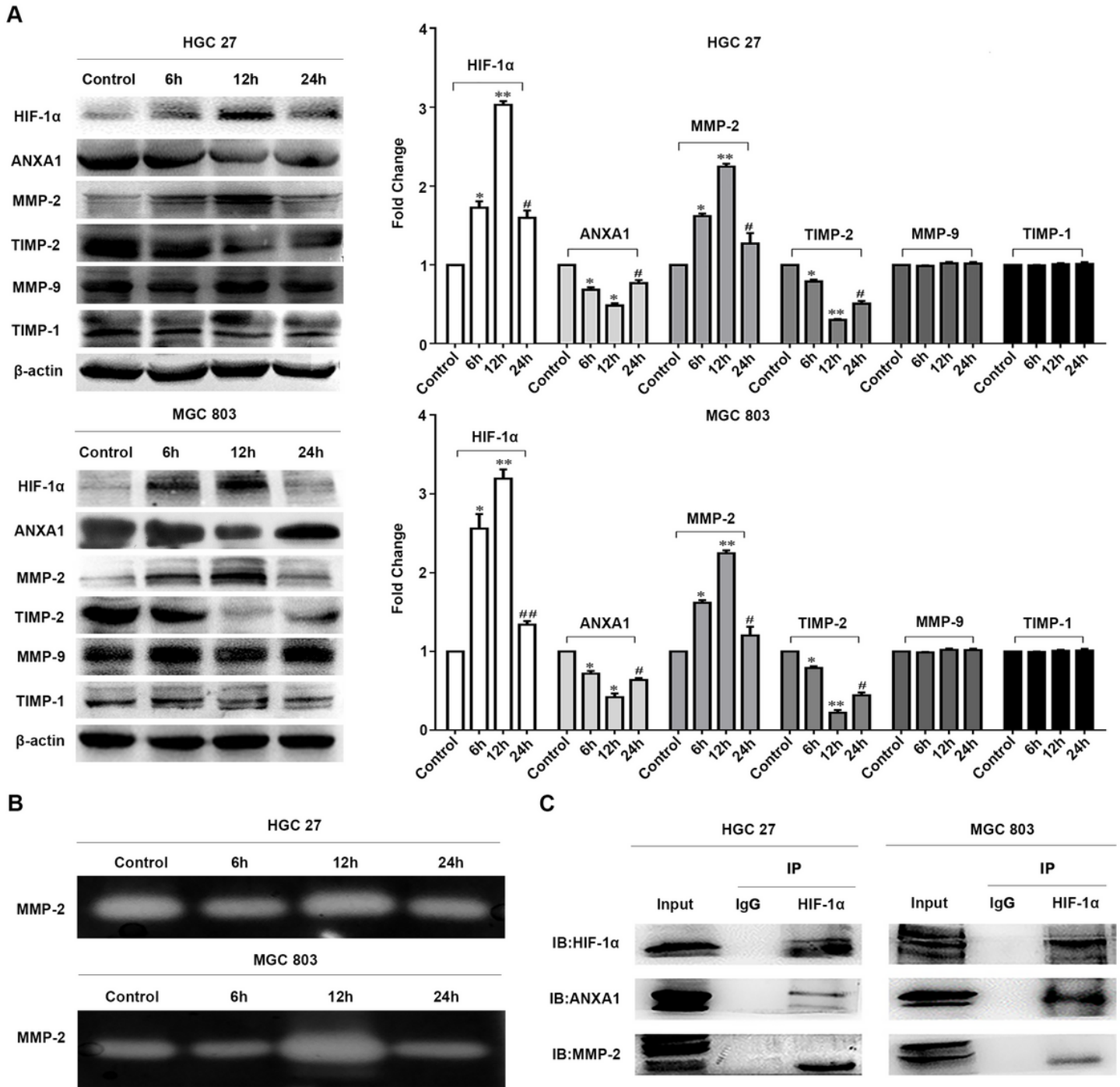


**Figure 4**

HIF-1 $\alpha$  improves migration and invasion of GC cells via regulating ANXA1/MMP-2 signaling. (A) Western blot analysis demonstrated the protein levels of HIF-1 $\alpha$ , ANXA1, MMP-2, TIMP-2, MMP-9 and TIMP-1 in HGC27 and MGC803 cells following 6, 12 and 24h co-cultured with CoCl<sub>2</sub>. Full-length blots are presented in Supplementary Fig 3A. (B) Gelatin zymography analysis of the activity of MMP-2. Full-length gels are presented in Supplementary Fig 3B. (C) Immunoprecipitation analysis of the interactions of HIF1 $\alpha$ , ANXA1 and MMP-2 in HGC27 and MGC803 cells.

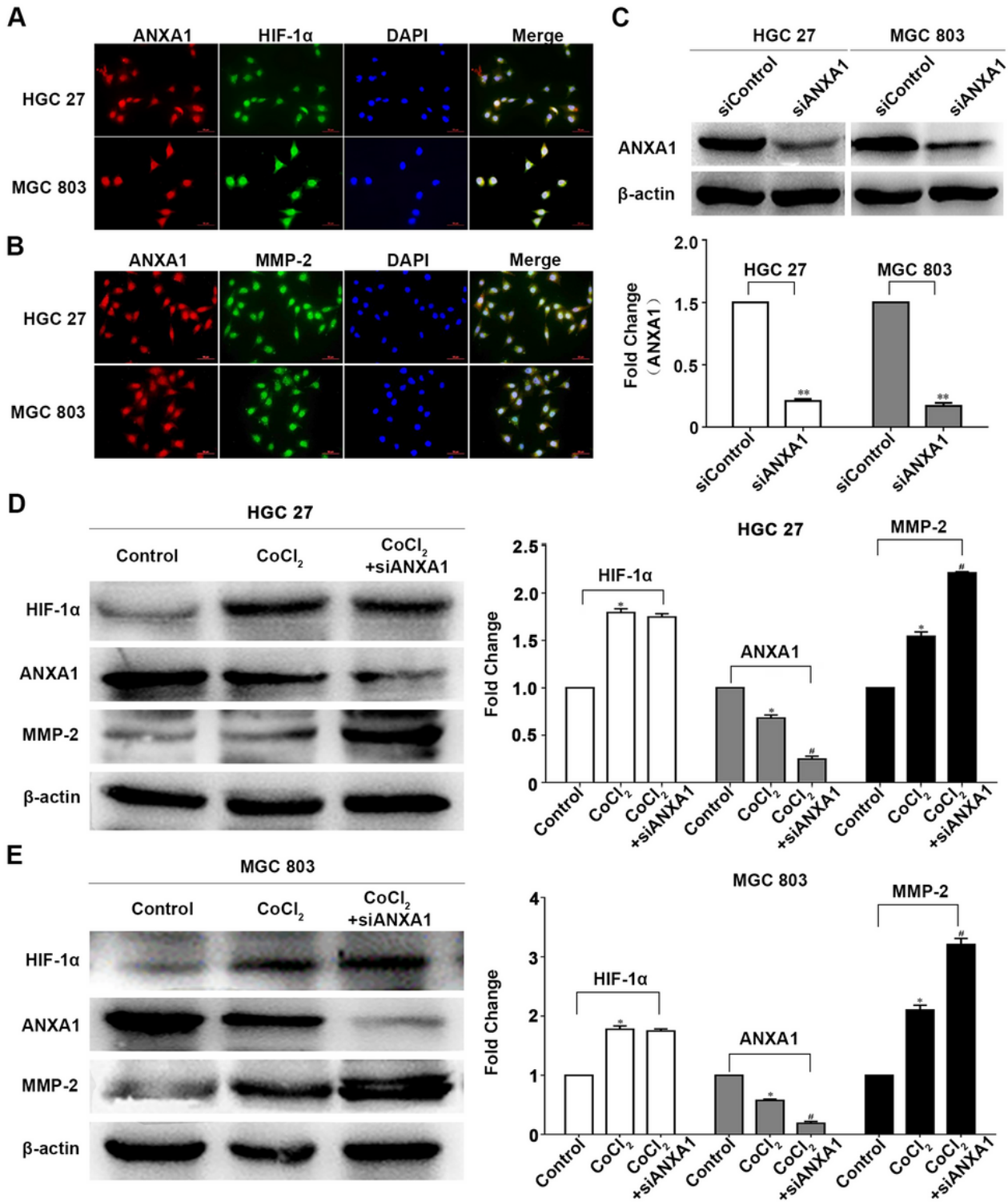


**Figure 5**

HIF1α regulated the expression of MMP-2 via ANXA1. Immunofluorescence staining identified the subcellular localization of HIF1α, ANXA1 and MMP-2 (A and B). The proteins (HIF1α, ANXA1 and MMP-2) are localized in the cytosol. NOTE: A. ANXA1 (red), HIF-1α (green), DAPI (blue); B. ANXA1 (red), MMP-2 (green), DAPI (blue). Original Magnification: ×40. (C) ANXA1 siRNA was transfected into GC cells. (D, E) The

expression of MMP-2 was upregulated after transfected ANXA1 siRNA in HGC27 and MGC803 cells under hypoxia condition.

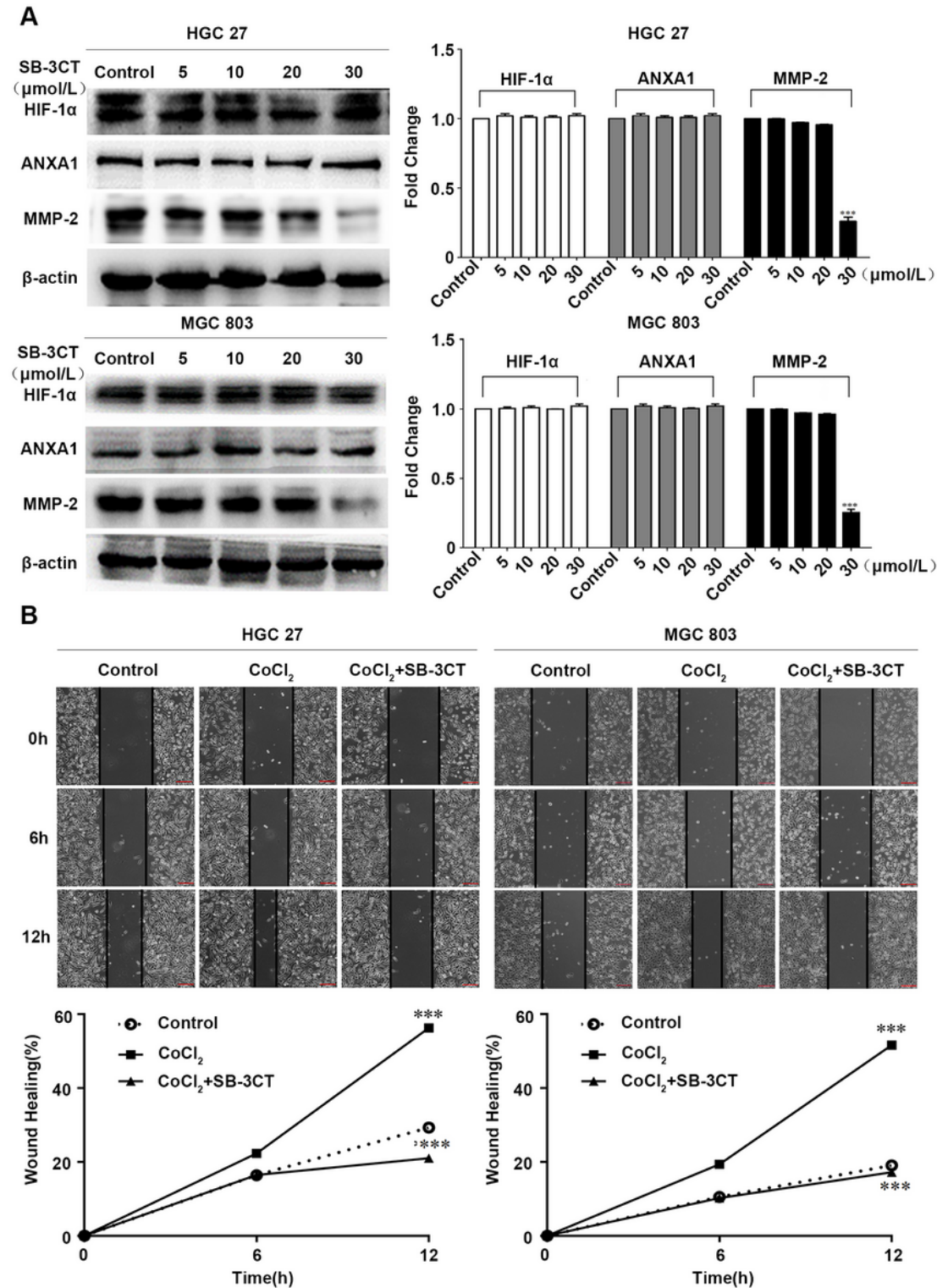


**Figure 6**

HIF1α regulated the migration and invasion of GC cells via HIF1α/ANXA1/MMP-2 pathway. (A) Western blot analysis: expressions of MMP-2 in HGC27 and MGC803 cells were down regulated by SB-3CT at 30 μmol/L. (B). The migration abilities were inhibited by SB-3CT in HGC27 and MGC803 cells at 12h.

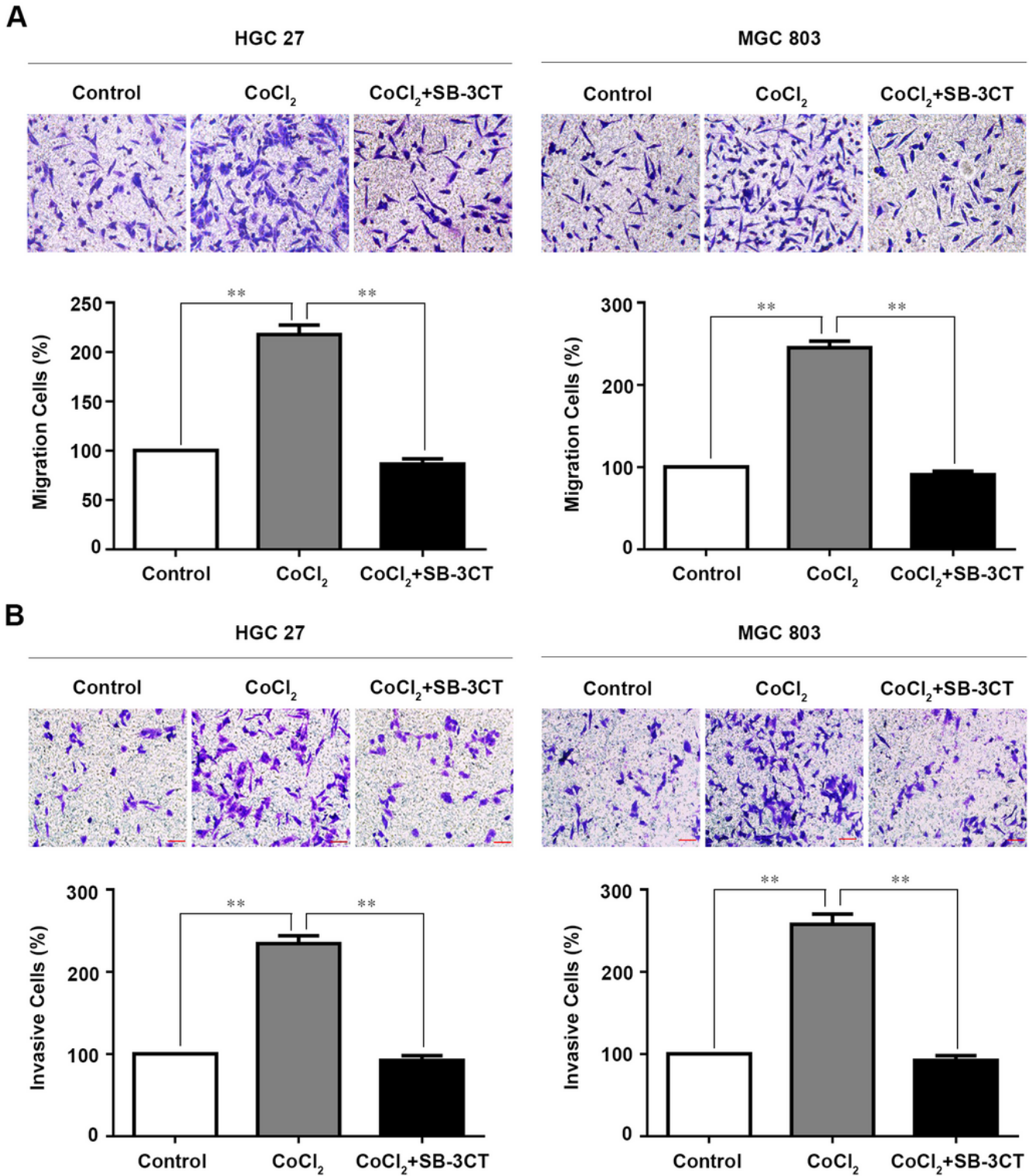


**Figure 7**

HIF1 $\alpha$  regulated the migration and invasion of GC cells via HIF1 $\alpha$ /ANXA1/MMP-2 pathway. (A) The migration abilities were inhibited by SB-3CT in HGC27 and MGC803 cells. (B) The invasion abilities were inhibited by SB-3CT in HGC27 and MGC803 cells.

## Supplementary Files

This is a list of supplementary files associated with this preprint. Click to download.

- [Supplementaryfile.docx](#)